IEEE Access
Multidisciplinary | Rapid Review | Open Access Journal

Date of publication xxxx 00, 0000, date of current version xxxx 00, 0000.

Digital Object Identifier 10.1109/ACCESS.2017.XXXXXXX

Initial Three-Dimensional Trajectory Design for Solar Sails using Bezier Shaping Approach

MINGYING HUO[1], ZE YU[1], HUI LIU[1,2], CE ZHAO[1], TONG LIN[1], ZHIGUO SONG[2], NAIMING QI[1]
[1] Department of Aerospace Engineering, Harbin Institute of Technology, Harbin 150001, China
[2] China Academy of Launch Vehicle Technology, Beijing 100076, China

Corresponding author: Naiming Qi (qinmok@163.com)

This work was supported in part by the National Natural Science Foundation of China under Grant Nos. 11672093 and 11702072, the China Postdoctoral Science Foundation under Grant No. 2017M611372, and the Heilongjiang Postdoctoral Fund under Grant No. LBH-Z16082.

ABSTRACT An approach for the fast generation of a minimum-time, three-dimensional trajectory for a spacecraft propelled by a solar sail with reflection control devices (RCDs) is presented using the authors' previously proposed Bezier curve-based shaping approach. In this approach, the time variation of the position components of the spacecraft are assumed in advance to follow Bezier curve functions. By optimizing a finite set of unknown coefficients defining the shape of the Bezier curves used to approximate the generic state variables, the boundary constraints and equations of motion are satisfied simultaneously under a time-optimized performance index. Unlike the thrust vector of a conventional electric thruster, that of an RCD-equipped solar sail is constrained. To consider the thrust characteristics of such solar sails, the propulsive acceleration inequality constraints were numerically investigated for an asteroid rendezvous. The simulation results demonstrate that the presented approach is able to design the transfer trajectory of a spacecraft propelled by an RCD-equipped solar sail in about 1% of the time required by the conventional Gauss pseudospectral method with comparable accuracy by considering the actual characteristics of the thrust vector. This allows for quick feasibility assessments of different solar sail spacecraft mission profiles during the preliminary mission design stage.

INDEX TERMS Solar sail, reflection control devices, Bezier curve, shape-based method.

I. INTRODUCTION

Regardless of whether an indirect or direct optimization method is used to determine spacecraft trajectory, a reasonable initial guess is required to determine the co-state or state variables [1], [2]. Because both indirect and direct optimization methods typically require considerable computational time, they are not suitable for quick feasibility assessments during the initial stages of mission design, when a large number of flight scenarios must be analyzed [3]. Therefore, a method for quick initial trajectory generation is of considerable significance for preliminary mission analysis and optimization of spacecraft with continuous-thrust propulsion systems [4], [5], [6]. Recently, quick trajectory generation techniques have been advanced using shape-based methods [7], in which the shape of the flight trajectory is assumed in advance to take the form of some specific function. The boundary constraints (BCs) and equations of motion (EoMs) are then simultaneously satisfied by computing some of the unknown coefficients in this assumed fixed function.

In 2004, Petropoulos and Longuski [7] first proposed the concept of a shape-based method for quick trajectory generation using an exponential sinusoidal shape to match the starting and finishing positions of a spacecraft. Patel et al. [8] applied a shape-based approach to the trajectory analysis and optimization of a spacecraft. More recently, a pseudo-equinoctial shaping method was introduced by Pascale and Vasile [9] for the initial trajectory design of low-thrust spacecraft using multiple gravity-assist. Wall and Conway [10] proposed an inverse polynomial (IP) method to satisfy the BCs of position and velocity. A hodographic-shaping method was proposed by Gondelach and Noomen [11] for the design of three-dimensional low-thrust interplanetary trajectories. Xie et al. [12] presented a lower-cost shaping method by considering the radial coordinate form of the initial and target orbits. A spherical shaping method, along with discussions on ways to improve upon the solution using tracking control, was presented by Novak and Vasile [13]. Xie et al. [14] presented a composite function shape-based method for the shaping approximation of low-thrust trajectories with large out-of-plane motion. To rapidly design

three dimensional low-thrust safe trajectories for spacecraft orbit transfer and rendezvous problems, Zeng et al. [15] proposed a shape-based analytic method. In order to approximate the evolution of pseudo-equinoctial elements for an asteroid rendezvous mission, Peloni et al. [16] introduced a shape-based method using a combination of exponential and sinusoidal terms. Vellutini and Avanzini [17] investigated low-thrust trajectories to cislunar Lagrangian point using shape-based method. Jiang et al. [18] introduced an improving low-thrust trajectory optimization method by adjoint estimation with shape-based path. Bassetto et al. [19] proposed using logarithmic spiral curve to describe the flight trajectory of the solar sail. More recently, Taheri and Abdelkhalik [20], [21] proposed a flexible method utilizing a finite Fourier series approximation to shape the flight trajectory in a two-dimensional plane. Later, the approximated trajectory was extended from two-dimensional to three-dimensional space [22], and the propulsive acceleration constraints of low-thrust engines with a thrust-handling feature were considered [23]. Huo et al. [24] applied this finite Fourier series shape-based method to realize quick initial trajectory generation for an electric solar wind sail.

Inspired by this recent research progress, a novel shape-based trajectory design method using a Bezier curve-based shaping approach was proposed in our previous research [25]. In this novel method, the time variations of the position components of the spacecraft are assumed in advance to follow Bezier curve functions [26]. For the rendezvous problem, the BCs can be satisfied concurrently by computing the twelve coefficients in the Bezier curve function. When there are three or fewer Bezier orders of approximation, the shape of the transfer trajectory is determined analytically from the BCs, and there is no unknown coefficient that must be optimized. This characteristic is similar to the radial coordinate form proposed by Xie et al. [12] and the inverse polynomial (IP) method proposed by Wall and Conway [10]. This type of method is suitable for the initial trajectory design of spacecraft propelled by low-thrust ion engines, whose thrust direction can be arbitrary. However, this type of method is not flexible enough to be used in the initial trajectory design of spacecraft with a thrust constraint, such as a spacecraft propelled by a solar sail [27], [28], [29], [30], [31], electric solar wind sail [32], [33], [34], [35], [36], [37], magnetic sail [38], [39], and etc. When there are more than three Bezier orders of coordinate approximation, the shape of the transfer trajectory cannot be determined analytically using only the BCs; there are unknown coefficients that need to be optimized to satisfy certain thrust constraints or to achieve optimal indexes. This property is similar to the Finite Fourier Series (FFS) method proposed by Abdelkhalik and Taheri [20], [21], [22], [23].

Solar sails equipped with a reflection control device (RCD) were demonstrated to be feasible during the Interplanetary Kite-craft Accelerated by Radiation Of the Sun (IKAROS) [40] mission. Since a solar sail with one RCD has one additional control variable than a traditional solar sail, it has attracted increasing attention in recent years. Mimasu et al. [41] investigated the orbit steering control of a spinning solar sail by mounting an RCD on the edge of the sail membrane to generate torque. Aliasi et al. [42] studied the artificial Lagrange points of a solar sail with an RCD. Mu et al. [43], [44] proposed the use of RCDs for orbit control and attitude-orbit control in the GeoSail Mission. Gong and Li applied solar sails with RCDs in Non-Keplerian orbits, such as the L2 Earth-Moon libration point [45], Halo orbit [46], and equilibria near asteroids [47]. The objective of this study was therefore to apply the previously proposed Bezier curve-based shaping approach in [25] to provide an efficient initial design for the three-dimensional interplanetary trajectory of a spacecraft propelled by an RCD-equipped solar sail.

In Section II of this paper, the orbital dynamics of the RCD-equipped solar sail are introduced. In Section III, the presented approach is applied to the fast generation of the minimum-time transfer trajectory of the RCD-equipped solar sail. In Section IV, the soundness of this method is verified by applying the presented approach to a simulated rendezvous mission with the asteroid 3671 Dionysus. Concluding remarks are then summarized in the final section.

II. ORBITAL DYNAMICS OF SOLAR SAILS WITH REFLECTION CONTROL DEVICES

A. COORDINATE SYSTEMS

In order to describe the orbital dynamics of this spacecraft, the heliocentric-ecliptic inertial frame $o_i - x_i y_i z_i$ and the orbital reference frame $o_o - x_o y_o z_o$ are introduced. As shown in Fig. 1, the origin o_i of the heliocentric-ecliptic inertial frame is located at the center-of-mass of the Sun, the x_i-axis is defined along the direction of the Sun equinox, the z_i-axis is normal to the ecliptic plane in the direction of Sun's north ecliptic pole, and the y_i-axis is oriented to form a right-handed system. The origin o_o of the orbital reference frame coincides with the center-of-mass of the spacecraft, the z_o-axis is along the Sun-spacecraft line, and the y_o-axis is perpendicular to the (z_o, z_i) plane in the same direction as the spacecraft inertial velocity.

In addition to these coordinate systems, a cylindrical reference frame (ρ, θ, z) is used to describe the position of the spacecraft in the proposed Bezier curve-based shaping approach. In this cylindrical reference frame, the coordinate ρ is the scalar projection of the Sun-spacecraft position vector on the ecliptic plane, coordinate z is along the z_i-axis of the heliocentric-ecliptic inertial frame, and coordinate θ is the polar angle, measured counterclockwise.

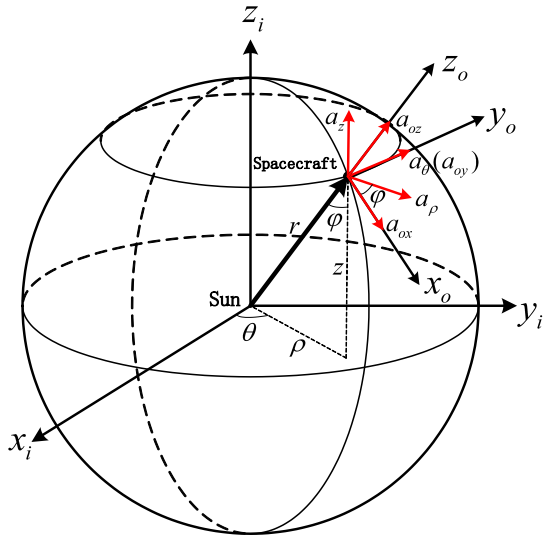

FIGURE 1. Cylindrical reference frame.

B. EQUATIONS OF MOTION

Consider a solar sail with a total area $A = A_1 + A_2$, where area A_1 absorbs all the sunlight and area A_2 reflects part of the sunlight. In A_2, the ratio of the reflected sunlight is given by η, where the remaining sunlight ($1-\eta$) is absorbed. In this paper, η is the ratio of reflected sunlight to total incident sunlight, and considered adjustable by controlling the input voltage of the electrochromic material of the RCD [42]. As discussed in [46], [47], the propulsive acceleration of the solar radiation pressure (SRP) on an RCD-equipped solar sail in $o_o - x_o y_o z_o$ can be written as follows:

$$\begin{bmatrix} a_{ox} \\ a_{oy} \\ a_{oz} \end{bmatrix} = a_c \left(\frac{r_\oplus}{r}\right)^2 \begin{bmatrix} (1-\upsilon)\eta\cos^2\alpha\sin\alpha\cos\gamma \\ (1-\upsilon)\eta\cos^2\alpha\sin\alpha\sin\gamma \\ (1-\eta+\upsilon\eta)\cos\alpha/2+(1-\upsilon)\eta\cos^3\alpha \end{bmatrix} \quad (1)$$

where $r = \sqrt{\rho^2 + z^2}$ is the distance between the Sun and the spacecraft; $r_\oplus \triangleq 1\text{au}$ is the average Sun–Earth distance; a_c is the characteristic acceleration of the solar-sail spacecraft, defined as the maximum value of the propulsive acceleration at a distance $r = r_\oplus$; $\upsilon = A_1 / A$ is the ratio of the absorbing area A_1 to the total area; $\eta \in [0,1]$ is the ratio of reflected sunlight to total sunlight in A_2; $\alpha \in [0, \pi/2]$ is the pitch angle measured from the sail normal vector to the Sun-spacecraft line, as seen in Fig. 2; the clock angle $\gamma \in [0, 2\pi]$ is the angle measured from the x_o -axis to the scalar projection of the sail normal vector in the (x_o, y_o) plane, as shown in Fig.2.

Considering the geometric relationship between the cylindrical reference frame and the orbital reference frame in Fig. 1, the propulsive acceleration of the solar sail described in the cylindrical reference frame is:

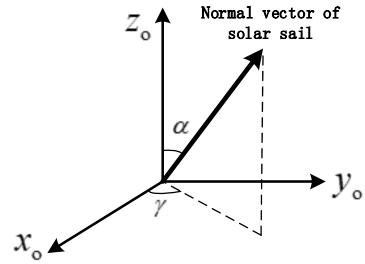

FIGURE 2. The pitch angle and the clock angle.

$$\begin{bmatrix} a_\rho \\ a_\theta \\ a_z \end{bmatrix} = \begin{bmatrix} \cos\varphi & 0 & \sin\varphi \\ 0 & 1 & 0 \\ -\sin\varphi & 0 & \cos\varphi \end{bmatrix} \begin{bmatrix} a_{ox} \\ a_{oy} \\ a_{oz} \end{bmatrix} = \begin{bmatrix} \cos\varphi a_{ox} + \sin\varphi a_{oz} \\ a_{oy} \\ -\sin\varphi a_{ox} + \cos\varphi a_{oz} \end{bmatrix} \quad (2)$$

where a_ρ, a_θ, a_z are the components of the solar sail propulsive acceleration in the cylindrical reference frame, $\cos\varphi = z/r$, and $\sin\varphi = \rho/r$.

Consequently, the EoMs of the spacecraft propelled by an RCD-equipped solar sail in the cylindrical reference frame are:

$$\begin{aligned} &\ddot{\rho} - \rho\dot{\theta}^2 + \mu_s \rho / r^3 = a_\rho \\ &\rho\ddot{\theta} + 2\dot{\rho}\dot{\theta} = a_\theta \\ &\ddot{z} + \mu_s z / r^3 = a_z \end{aligned} \quad (3)$$

where μ_s is the parameter coefficient of the Sun.

III. BEZIER CURVE-BASED TRAJECTORY SHAPING APPROACH

A. STATES APPROXIMATION

In the Bezier curve-based trajectory shaping approach proposed in [25], the approximations of orbital coordinates (ρ, θ, z) are expanded by applying a Bezier curve function as follows:

$$\begin{aligned} \rho(\tau) &= \sum_{j=0}^{n_\rho} B_{\rho,j}(\tau) P_{\rho,j} \\ \theta(\tau) &= \sum_{j=0}^{n_\theta} B_{\theta,j}(\tau) P_{\theta,j} \\ z(\tau) &= \sum_{j=0}^{n_z} B_{z,j}(\tau) P_{z,j} \end{aligned} \quad (4)$$

where $0 \le \tau = t/T \le 1$ is the scaled time, T is the total flight time; n_ρ, n_θ, and n_z are the orders of the Bezier curve function for each coordinate; $P_{\rho,j}(j \in [0, n_\rho])$, $P_{\theta,j}(j \in [0, n_\theta])$, and $P_{z,j}(j \in [0, n_z])$ are the Bezier coefficients; $B_{\rho,j}(\tau)$, $B_{\theta,j}(\tau)$, and $B_{z,j}(\tau)$ are the Bezier basis functions for the approximations of state variables, which can be written as:

$$
\begin{aligned}
B_{\rho,j}(\tau) &= \frac{n_\rho!}{j!(n_\rho-j)!}\tau^j(1-\tau)^{n_\rho-j} \qquad j\in[0,n_\rho]\\
B_{\theta,j}(\tau) &= \frac{n_\theta!}{j!(n_\theta-j)!}\tau^j(1-\tau)^{n_\theta-j} \qquad j\in[0,n_\theta]\\
B_{z,j}(\tau) &= \frac{n_z!}{j!(n_z-j)!}\tau^j(1-\tau)^{n_z-j} \qquad j\in[0,n_z]
\end{aligned} \tag{5}
$$

In a general three-dimensional rendezvous problem, approximations of the orbital coordinates are required to satisfy the following twelve BCs:

$$
\begin{aligned}
&\rho(\tau=0)=\rho_i \qquad \rho(\tau=1)=\rho_f\\
&\rho'(\tau=0)=T\dot\rho_i \qquad \rho'(\tau=1)=T\dot\rho_f\\
&\theta(\tau=0)=\theta_i \qquad \theta(\tau=1)=\theta_f\\
&\theta'(\tau=0)=T\dot\theta_i \qquad \theta'(\tau=1)=T\dot\theta_f\\
&z(\tau=0)=z_i \qquad z(\tau=1)=z_f\\
&z'(\tau=0)=T\dot z_i \qquad z'(\tau=1)=T\dot z_f
\end{aligned} \tag{6}
$$

where the superscript '·' represents the derivative with respect to time t; the superscript '′' denotes the derivative with respect to scaled time τ; and subscripts 'i' and 'f' respectively indicate the initial and final conditions.

To avoid repetition, this paper only presents the processing approach for coordinate ρ; the other two coordinates (θ and z) can be processed in a similar way. According to Eq. (4), the first τ-derivative of the coordinate ρ approximation is:

$$
\rho'(\tau)=\sum_{j=0}^{n_\rho}B'_{\rho,j}(\tau)P_{\rho,j} \tag{7}
$$

where $B'_{\rho,j}(\tau)$ is the first τ-derivative of the Bezier basis function for the coordinate ρ approximation, and can be obtained according to Eq. (5) as:

$$
B'_{\rho,j}(\tau)=\begin{cases}
-n_\rho(1-\tau)^{n_\rho-1} & j=0\\
\dfrac{n_\rho!}{(j-1)!(n_\rho-j)!}\tau^{j-1}(1-\tau)^{n_\rho-j} & j\in[1,n_\rho-1]\\
-\dfrac{n_\rho!}{j!(n_\rho-j-1)!}\tau^j(1-\tau)^{n_\rho-j-1} & \\
n_\rho\tau^{n_\rho-1} & j=n_\rho
\end{cases} \tag{8}
$$

Substituting τ=0 and τ=1 into Eqs. (5) and (8), we can determine the characteristics of the Bezier basis function at the boundary as:

$$
\begin{aligned}
B_{\rho,j}(\tau=0)&=\begin{cases}1 & j=0\\ 0 & j\in[1,n_\rho]\end{cases}\\
B_{\rho,j}(\tau=1)&=\begin{cases}0 & j\in[0,n_\rho-1]\\ 1 & j=n_\rho\end{cases}\\
B'_{\rho,j}(\tau=0)&=\begin{cases}-n_\rho & j=0\\ n_\rho & j=1\\ 0 & j\in[2,n_\rho]\end{cases}\\
B'_{\rho,j}(\tau=1)&=\begin{cases}0 & j\in[0,n_\rho-2]\\ -n_\rho & j=n_\rho-1\\ n_\rho & j=n_\rho\end{cases}
\end{aligned} \tag{9}
$$

Considering the approximation functions (Eq. (5) and Eq. (8)) and BCs (Eq. (6)), we can obtain the following coordinate equations:

$$
\begin{aligned}
\rho_i &= \rho(\tau=0)=P_{\rho,0}\\
\rho_f &= \rho(\tau=1)=P_{\rho,n_\rho}\\
T\dot\rho_i &= \rho'(\tau=0)=n_\rho(P_{\rho,1}-P_{\rho,0})\\
T\dot\rho_f &= \rho'(\tau=1)=n_\rho(P_{\rho,n_\rho}-P_{\rho,n_\rho-1})
\end{aligned} \tag{10}
$$

Consequently, the four Bezier coefficients $P_{\rho,0}$, $P_{\rho,1}$, $P_{\rho,n_\rho-1}$, and P_{ρ,n_ρ} in the coordinate ρ approximation can be determined by the BCs as follows:

$$
\begin{aligned}
P_{\rho,0} &= \rho_i\\
P_{\rho,1} &= \rho_i+T\dot\rho_i/n_\rho\\
P_{\rho,n_\rho-1} &= \rho_f-T\dot\rho_f/n_\rho\\
P_{\rho,n_\rho} &= \rho_f
\end{aligned} \tag{11}
$$

The overall objective of this paper is to use the proposed method find a feasible trajectory that could be tracked by an RCD-equipped solar sail. Thus, it is necessary to evaluate the motion at a selection of discretized points. The Legendre–Gauss (LG) distribution of the discretization points, defined as the roots of the mth-degree Legendre polynomial, is adopted in this paper to this end as follows:

$$
0=\tau_1<\tau_2<\cdots<\tau_{m-1}<\tau_m=1 \tag{12}
$$

As the scaled-time vectors are expressed as column vectors, their coordinates and associated first and second τ-derivatives can be shown in compact matrix notation form as follows, still taking coordinate ρ as an example:

$$
\begin{aligned}
[\rho]_{m\times1} &= [B_\rho]_{m\times(n_\rho+1)}[P_\rho]_{(n_\rho+1)\times1}\\
[\rho']_{m\times1} &= [B'_\rho]_{m\times(n_\rho+1)}[P_\rho]_{(n_\rho+1)\times1}\\
[\rho'']_{m\times1} &= [B''_\rho]_{m\times(n_\rho+1)}[P_\rho]_{(n_\rho+1)\times1}
\end{aligned} \tag{13}
$$

where $[P_\rho]_{(n_\rho+1)\times1}=[P_{\rho,0}\quad P_{\rho,1}\quad [X_\rho]^T_{(n_\rho-3)\times1}\quad P_{\rho,n_\rho-1}\quad P_{\rho,n_\rho}]^T$ are the Bezier coefficients. Note that $P_{\rho,0}$, $P_{\rho,1}$, $P_{\rho,n_\rho-1}$, and

P_{ρ,n_ρ} are the known coefficients determined by the BCs, and $[X_\rho]_{(n_\rho-3)\times 1}=[P_{\rho,2} \ \cdots \ P_{\rho,n_\rho-2}]^T$ are the unknown coefficients that need to be optimized. Matrices $[B_\rho]_{m\times(n_\rho+1)}$, $[B'_\rho]_{m\times(n_\rho+1)}$, and $[B''_\rho]_{m\times(n_\rho+1)}$ can be calculated by substituting discretization points $[\tau_{APP}]_{m\times 1}$ into the coordinate approximations and their τ-derivatives.

Once the orders of Bezier curve functions n_ρ, n_θ, and n_z, and the number of discretization points (m) are given, the coefficient matrices are constant. Therefore, the coefficient matrices can be calculated once and stored, and then used in each iteration of optimization. Since this obviates the need to re-compute the coefficient matrix for each iteration, the computation load is effectively reduced. The coefficient matrices are constructed as:

$$
\begin{aligned}
[B_\rho]_{m\times(n_\rho+1)}&=\begin{bmatrix} B_{\rho,0}(\tau_1) & \cdots & B_{\rho,n_\rho}(\tau_1) \\ \vdots & \ddots & \vdots \\ B_{\rho,0}(\tau_m) & \cdots & B_{\rho,n_\rho}(\tau_m) \end{bmatrix} \\
[B'_\rho]_{m\times(n_\rho+1)}&=\begin{bmatrix} B'_{\rho,0}(\tau_1) & \cdots & B'_{\rho,n_\rho}(\tau_1) \\ \vdots & \ddots & \vdots \\ B'_{\rho,0}(\tau_m) & \cdots & B'_{\rho,n_\rho}(\tau_m) \end{bmatrix} \\
[B''_\rho]_{m\times(n_\rho+1)}&=\begin{bmatrix} B''_{\rho,0}(\tau_1) & \cdots & B''_{\rho,n_\rho}(\tau_1) \\ \vdots & \ddots & \vdots \\ B''_{\rho,0}(\tau_m) & \cdots & B''_{\rho,n_\rho}(\tau_m) \end{bmatrix}
\end{aligned} \tag{14}
$$

If $n_\rho=n_\theta=n_z=3$, the shape of the flight trajectory can be determined analytically using the twelve BCs, and there is no unknown coefficient that must be optimized. If $n_\rho>3, n_\theta>3, n_z>3$, the shape of the flight trajectory cannot be determined analytically by the BCs because unknown coefficients $[X_\rho]_{(n_\rho-3)\times 1}$, $[X_\theta]_{(n_\theta-3)\times 1}$, and $[X_z]_{(n_z-3)\times 1}$ need to be optimized to satisfy certain thrust constraints and achieve optimal indexes. This is similar to the FFS method proposed by Abdelkhalik and Taheri [20], [21], [22], [23]. This type of method is sufficiently flexible to be used for a quick trajectory generation of a solar-sail propelled spacecraft. For a fixed transfer time-problem, the coefficient matrices in both the Bezier curve-based shaping and FFS methods are constant matrices when the number of Fourier terms and discretization points are given. Still, for a free transfer time-problem, some of the matrices in the FFS method need to be calculated within each iteration, but this is not required in the proposed Bezier curve method.

Considering the matrix representations of coordinates (ρ, θ, z) and related first and second τ-derivatives, the propulsive acceleration component equations can be obtained in the form of compact matrices, with reference to Eq. (3), based on the principle of inverse dynamics as follows:

$$
\begin{aligned}
[a_\rho]_{m\times 1}&=a_\rho([\rho]_{m\times 1},[z]_{m\times 1},[\theta']_{m\times 1},[\rho'']_{m\times 1}) \\
[a_\theta]_{m\times 1}&=a_\theta([\rho]_{m\times 1},[\rho']_{m\times 1},[\theta']_{m\times 1},[\theta'']_{m\times 1}) \\
[a_z]_{m\times 1}&=a_z([\rho]_{m\times 1},[z]_{m\times 1},[z'']_{m\times 1})
\end{aligned} \tag{15}
$$

B. NONLINEAR OPTIMIZATION PROBLEM

Unlike an electric thruster (i.e., a continuous thrust ion engine), the propulsive acceleration vector of an RCD-equipped solar sail is constrained as discussed in [46] and [47]. To accurately account for the thrust characteristics of such a solar sail, the inequality constraints on the thrust direction need to be derived according to the relevant thrust model. To obtain the analytical forms of the control quantities, the acceleration model needs to be appropriately simplified as follows:

$$
\begin{bmatrix} a_{ox} \\ a_{oy} \\ \hat{a}_{oz} \end{bmatrix}=a_c\left(\frac{r_0}{r}\right)^2\begin{bmatrix} (1\text{-}\upsilon)\hat{\eta}\cos^2\hat{\alpha}\sin\hat{\alpha}\cos\hat{\gamma} \\ (1\text{-}\upsilon)\hat{\eta}\cos^2\hat{\alpha}\sin\hat{\alpha}\sin\hat{\gamma} \\ (1-\upsilon)\hat{\eta}\cos^3\hat{\alpha} \end{bmatrix} \tag{16}
$$

where $\hat{a}_{oz}$ denotes the simplification of a_{oz}, and $\hat{\eta},\hat{\alpha},\hat{\gamma}$ are control variables in the simplified thrust model.

According to the simplified thrust model in Eq. (16), the analytical representations of the control variables can be written as:

$$
\begin{aligned}
\hat{\alpha}&=\text{acos}\left(\frac{\hat{a}_{oz}}{\sqrt{a_{ox}^2+a_{oy}^2+\hat{a}_{oz}^2}}\right) \\
\hat{\gamma}&=\text{atan}\left(\frac{a_{oy}}{a_{ox}}\right) \\
\hat{\eta}&=\frac{\left(a_{ox}^2+a_{oy}^2+\hat{a}_{oz}^2\right)^{3/2}}{a_c(1-\upsilon)\left(r_0/r\right)^2\hat{a}_{oz}^2}
\end{aligned} \tag{17}
$$

Considering the coordinate transformation relationship between the cylindrical reference frame and orbital reference frame expressed in Eq. (2) and the matrix form of the propulsive acceleration components shown in Eq. (15), Eq. (17) can be written as:

$$
\begin{aligned}
[\hat{\alpha}]_{m\times 1}&=a\cos\left(\frac{\sin[\varphi]\cdot[a_\rho]+\cos[\varphi]\cdot[a_z]}{\sqrt{D}}\right) \\
[\hat{\gamma}]_{m\times 1}&=a\tan\left(\frac{a_\theta}{\cos[\varphi]\cdot[a_\rho]-\sin[\varphi]\cdot[a_z]}\right) \\
[\hat{\eta}]_{m\times 1}&=\frac{(D)^{3/2}}{a_c(1-\upsilon)\left(\frac{r_0}{[r]}\right)^2\left(\sin[\varphi]\cdot[a_\rho]+\cos[\varphi]\cdot[a_z]\right)^2}
\end{aligned} \tag{18}
$$

where:

$$
\begin{aligned}
D&=(\cos[\varphi]\cdot[a_\rho]-\sin[\varphi]\cdot[a_z])^2+([a_\theta])^2 \\
&\quad+(\sin[\varphi]\cdot[a_\rho]+\cos[\varphi]\cdot[a_z])^2>0
\end{aligned}
$$

Considering $\eta \in [0,1]$, $2m$ inequality constraints, $[\hat{\eta}]_{m\times 1} \geq 0$ and $[\hat{\eta}]_{m\times 1} \leq 1$, can be obtained. Additionally, because the angle between the thrust direction of the solar sail and the incident direction of the sunlight must be acute, the propulsive acceleration component $[\hat{a}_{oz}]_{m\times 1}$ is always greater than zero. In general spacecraft trajectory optimization problems, the optimization performance index is usually defined as the shortest flight time or the least fuel consumption. Considering that a solar sail harnesses solar light pressure to generate continuous thrust without consuming fuel, and assuming that the energy consumed by the spacecraft management system, thermal control system, attitude control system, etc. is completely provided by solar panels, the flight time is usually selected as the performance index to be optimized. By analyzing a finite number of LG discretization points, the continuous trajectory optimization problem can be transformed into the following small-scale nonlinear programming problem (NLP):

$$\begin{aligned} &\min \quad T \\ &[X_\rho],[X_\theta],[X_z],T \\ &\text{s.t.} \quad 0 \leq [\hat{\eta}]_{m\times 1} \leq 1, [\hat{a}_{oz}]_{m\times 1} \geq 0 \end{aligned} \tag{19}$$

where T is the total flight time, and $[X_\rho]_{(n_\rho-3)\times 1}$, $[X_\theta]_{(n_\theta-3)\times 1}$, and $[X_z]_{(n_z-3)\times 1}$ are the unknown Bezier coefficients for each coordinate approximation. For the free-time problem of orbital transfer, a total of $n_\rho + n_\theta + n_z - 8$ variables need to be optimized, including the total flight time T and all the unknown Bezier coefficients for each coordinate.

The basic idea of the variable initialization technique used to initialize the unknown coefficients is to provide an approximation of the coordinates (ρ, θ, z) at m LG discretization points. Then, the unknown coefficients can be calculated by fitting the considered Bezier curve functions to this set of discrete points, as discussed in detail in [25].

IV. NUMERICAL RESULTS

To verify the effectiveness of the proposed Bezier curve-based shaping approach in establishing the trajectory of RCD-equipped solar sails, an initial three-dimensional trajectory generation for a rendezvous with the asteroid 3671 Dionysus was conducted. The selected asteroid is a difficult target as it exhibits considerable variations in inclination and eccentricity. Moreover, the applicability of the obtained solutions as direct solutions was evaluated by using them as an initial guess for a Gauss pseudospectral method (GPM) [48] solver. For the initial three-dimensional trajectory design of this simulation using the proposed Bezier approach, the orders of the Bezier curve function and the number of LG discrete points were selected as n_ρ=n_θ=n_z=16 and m=40, respectively. The interior point method was then used to solve the small-scale NLP, which was transformed from the Bezier shaping approach. In the GPM-based trajectory optimization, 60 LG points were established and the NLP was then solved using sequential quadratic programming. Both the interior point method and the sequential quadratic programming method were implemented using the MATLAB *fmincon* function. Additionally, the ratio υ=A_1 / A was assumed to be zero in this simulation, meaning that there is no uncontrollable material in the solar sail that absorbs all the sunlight. All simulations were conducted on a personal computer with a 2.2 GHz Intel Core i5-5200U CPU and 8.00 GB of RAM.

A. EARTH-DIONYSUS TRANSFER WITH FIXED MAXIMUM ACCELERATION

Assuming a spacecraft propelled by a solar sail with a characteristic acceleration of $a_c = 1\text{mm/s}^2$ is launched on 20 March 2024 (also selected using the optimization procedure), the initial Earth–Dionysus trajectory generated using the presented Bezier approach and optimized trajectory obtained by the GPM are shown in Figure 3. In this mission scenario, the total transfer time obtained using the Bezier approach was 1078.610 days whereas that obtained using the GPM was 1071.111 days, constituting a minor difference of approximately 0.7%. More notably, however, the computational time required to generate the initial trajectory using the Bezier approach was 80.514 s, just ~1.00% of that required to generate and optimize the trajectory using the GPM (8027.740 s).

The three components of the solar-sail spacecraft position and velocity vectors (in $o_i - x_i y_i z_i$) obtained using the Bezier approach and GPM are shown in Figures 4 and 5. It can be observed that the position vectors and velocity vectors generated by both the Bezier approach and GPM are able to meet the BCs quite well, indicating that the spacecraft successfully entered the sphere of influence for Dionysus at a low relative velocity.

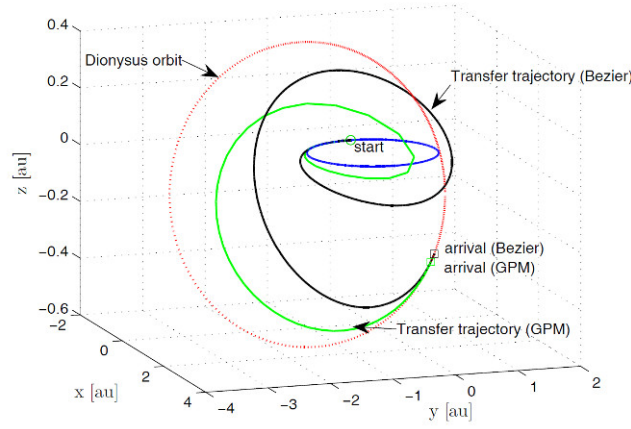

FIGURE 3. Optimal Earth–Dionysus transfer trajectories obtained using the Bezier curve-based shaping approach and the GPM with $a_c = 1\text{mm/s}^2$.

Noted that control variables (η, α, γ) were calculated using $\hat{\eta}, \hat{\alpha}, \hat{\gamma}$ by the following optimization procedure: the propulsive acceleration $[a_{ox}, a_{oy}, a_{oz}]^{\mathrm{T}}$ can be calculated by using $\hat{\eta}, \hat{\alpha}, \hat{\gamma}$ according to Eq. (16), in which a_{oz} is forced to

equal the simplified acceleration component $\hat{a}_{oz}$. Then, the control variables (η, α, γ) can be obtained according to Eq. (1). The components of the propulsive acceleration vector $(o_o - x_o y_o z_o)$ obtained using the proposed Bezier approach are shown in Figure 6. It is notable that thrust component a_{oz} is always greater than zero. The time histories of the reflection ratio η and thrust angles $(\alpha,\ \gamma)$ are illustrated in Figure 7. The time histories of the control angles obtained using the Bezier approach and the GPM are both smooth and continuous, which is of considerable benefit to the solar sail attitude tracking control. All of the inequality constraints on the thrust of the RCD-equipped solar sail described in Eq. (19) are satisfied.

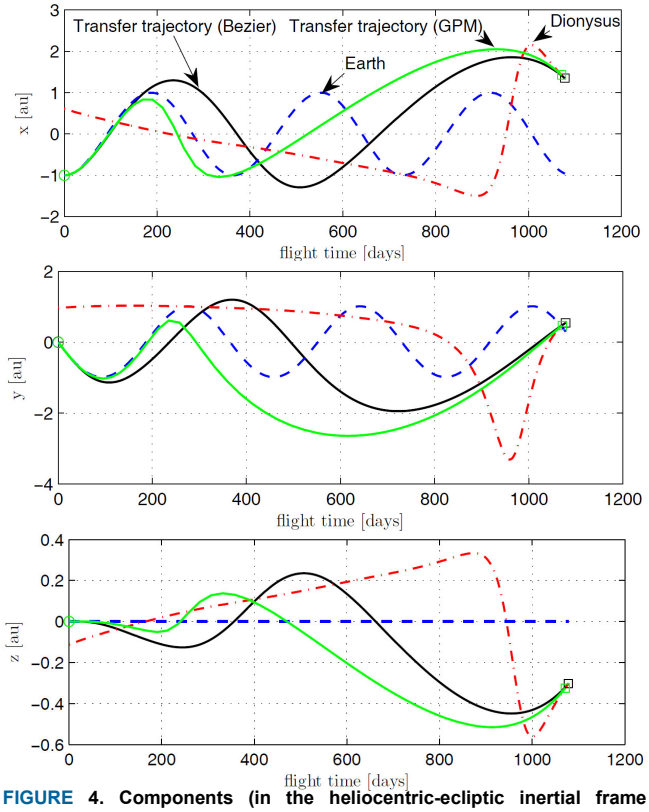

FIGURE 4. Components (in the heliocentric-ecliptic inertial frame $o_i - x_i y_i z_i$) of the position vectors for an optimal Earth–Dionysus transfer using the Bezier curve-based shaping approach and the GPM with $a_c = 1\text{mm/s}^2$.

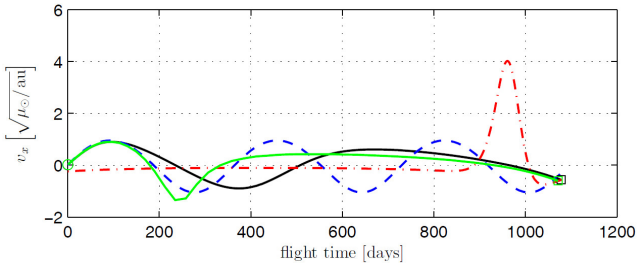

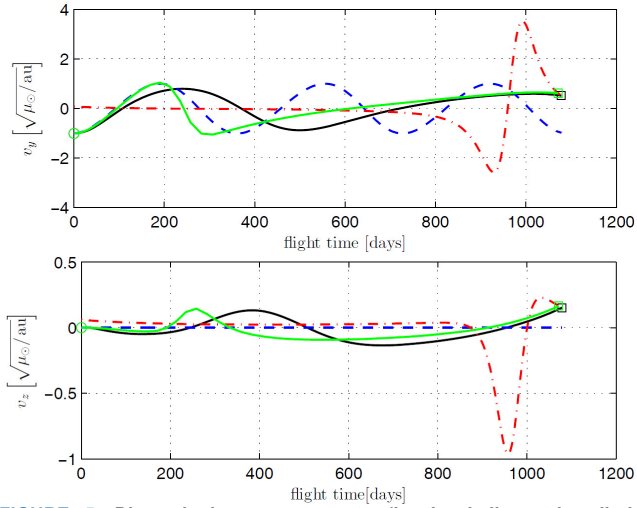

FIGURE 5. Dimensionless components (in the heliocentric-ecliptic inertial frame $o_i - x_i y_i z_i$) of the velocity vectors for an optimal Earth–Dionysus transfer using the Bezier curve-based shaping approach and the GPM with $a_c = 1\text{mm/s}^2$.

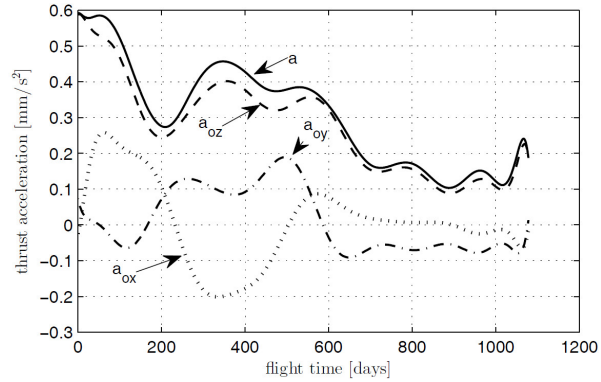

FIGURE 6. Components (in $o_o - x_o y_o z_o$) of the propulsive acceleration vector for an optimal Earth–Dionysus transfer using the Bezier curve-based shaping approach with $a_c = 1\text{mm/s}^2$.

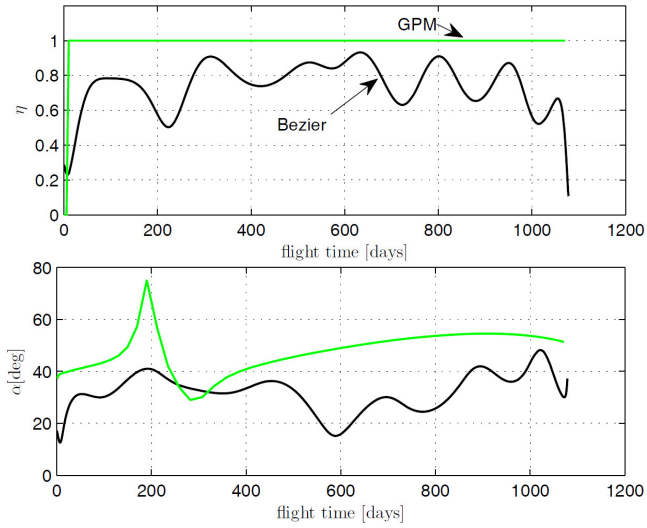

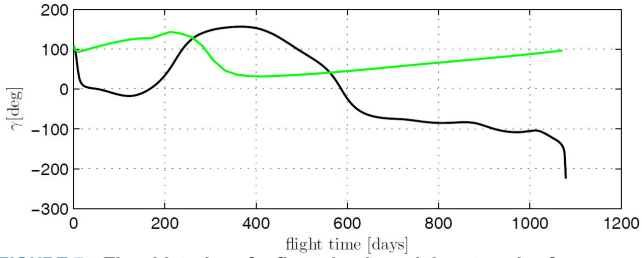

FIGURE 7. Time histories of reflected ratio and thrust angles for an optimal Earth–Dionysus transfer using the Bezier curve-based shaping approach and the GPM with $a_c = 1\text{mm/s}^2$.

B. EARTH-DIONYSUS TRANSFERS WITH DIFFERENT MAXIMUM ACCELERATIONS

The optimal transfer times and computational times for Earth-Dionysus scenario are summarized in Table 1, when the characteristic acceleration of a solar sail varies in the range $a_c \in [0.6,1.0]\text{mm/s}^2$. Simulation results show that the optimal transfer time increases with decreasing a_c, and the average difference between the optimal flight times obtained by Bezier approach and GPM is only approximately 0.82%. However, the average computational time used to generate the initial trajectory by using Bezier approach is approximately 1.14% of the average computational time used to further optimize the trajectory by using GPM.

TABLE 1. Transfer times and computational times for Earth-Dionysus.

$a_c[\text{mm/s}^2]$	Transfer time [days]		Computational time [s]	
	Bezier	GPM	Bezier	GPM
0.6	1294.48	1280.38	91.373	7653.868
0.7	1158.74	1148.04	87.636	7415.372
0.8	1120.32	1111.75	88.267	6247.650
0.9	1090.19	1083.79	78.452	7980.298
1.0	1078.61	1071.11	80.514	8027.740

V. CONCLUSION

The rapid generation of a minimum-time, three-dimensional trajectory for a spacecraft propelled by a solar sail equipped with an RCD using the previously proposed Bezier curve-based shaping approach is demonstrated in this paper. In this shaping approach, the time variation of the spacecraft position components are assumed in advance to follow Bezier curve functions. To accurately consider the features of the thrust produced by an RCD-equipped solar sail, the inequality constraints on propulsive acceleration were studied. To verify the effectiveness of the Bezier curve-based shaping approach in application to the trajectory of spacecraft propelled by RCD-equipped solar sails, an initial three-dimensional trajectory design for a rendezvous with the asteroid 3671 Dionysus was performed. The numerical simulation shows that the Bezier approach can be used to quickly generate a reasonable three-dimensional initial trajectory for the solar sail-propelled spacecraft. Importantly, all of the inequality thrust constraints of the RCD-equipped solar sail were satisfied. The objective function produced by the Bezier curve-based shaping approach differs from the objective function produced by the GPM by only about 0.8%, but takes merely ~1% of the time to generate, representing a considerable savings in computational time and resources, which is of particular benefit during preliminary mission design stages. In addition, it is noteworthy that the results obtained by Bezier shaping approach are infinitely continuous described by functions of time, while those obtained by GPM are finite discrete points.

REFERENCES

[1] J. T. Betts, "Survey of numerical methods for trajectory optimization," *J. Guid. Control Dynam.*, vol. 21, no. 2, pp. 193-207, Mar. 1998, doi: 10.2514/2.4231.

[2] B. A. Conway, "A survey of method available for the numerical optimization of continuous dynamic systems," *J. Optimiz. Theory App.*, vol. 152, no. 2, pp. 271-306, Feb. 2012, doi: 10.1007/s10957-011-9918-z.

[3] M. Di Carlo, J. M. Romero Martin, and M. Vasile, "Automatic trajectory planning for low-thrust active removal mission in low-Earth orbit," *Adv. Space Res.*, vol. 59, no. 5, pp. 1234-1258, Mar. 2017, doi: 0.1016/j.asr.2016.11.033.

[4] S. Li, Y. Zhu and Y. Wang, "Rapid design and optimization of low-thrust rendezvous/interception trajectory for asteroid detection missions," *Adv. Space Res*., vol. 53, no. 4, pp.696-707, Feb. 2014, doi: 10.1016/j.asr.2013.12.012.

[5] M. Saghamanesh, and H. Baoyin, "A robust homotopic approach for continuous variable low-thrust trajectory optimization," *Adv. Space Res*., vol. 62, no. 11, pp. 3095-3113, Dec. 2018, doi: 10.1016/j.asr.2018.08.046.

[6] Y. Gao, X. Lu, Y. Peng, B. Xu, and T. Zhao, "Trajectory optimization of multiple asteroids exploration with asteroid 2010TK7 as main target," *Adv. Space Res.*, vol. 63, no. 1, pp. 432-442, Jan. 2019, doi: 10.1016/j.asr.2018.08.047.

[7] A.E. Petropoulos, and J.M. Longuski, "Shape-based algorithm for the automated design of low-thrust gravity assist trajectories," *J. Spacecraft Rockets*, vol. 41, no. 5, pp. 787-796, Sep. 2004, doi: 10.2514/1.13095.

[8] P. Patel, D. Scheers, and T. Zurbruchen, "A shape based approach to spacecraft trajectories: analysis and optimization," *Advances in the Astronautical Sciences*, vol. 120, no. 1-2, pp. 445-463, Jan. 2005.

[9] P. De Pascale, and M. Vasile, "Preliminary design of low-thrust multiple gravity-assist trajectories," *J. Spacecraft Rockets*, vol. 43, no. 5, pp. 1069-1076, Sep. 2006, doi: 10.2514/1.19646.

[10] B. J. Wall, and B. A. Conway, "Shape-based approach to low-thrust rendezvous trajectory design," *J. Guid. Control Dynam*., vol. 32, no. 1, pp. 95-101, Jan. 2009, doi: 10.2514/1.36848.

[11] D.J. Gondelach, and R. Noomen, "Hodographic-shaping method for low-thrust interplanetary trajectory design," *J. Spacecraft Rockets*, vol. 52, no. 3, pp. 728-738, May. 2015, doi:10.2514/1.A32991.

[12] C. Xie, G. Zhang, and Y. Zhang, "Simple shaping approximation for low-thrust trajectories between coplanar elliptical orbits," *J. Guid. Control Dynam.*, vol. 38, no. 12, pp. 2448-2454, Dec. 2015, doi: 10.2514/1.G001209.

[13] D. M. Novak, and M. Vasile, "Improved shaping approach to the preliminary design of low-thrust trajectories," *J. Guid. Control Dynam.*, vol. 34, no. 1, pp. 128-147, Jan. 2011, doi: 10.2514/1.50434.

[14] C. Xie, G. Zhang, and Y. Zhang, "Shaping approximation for low-thrust trajectories with large out-of-plane motion," *J. Guid. Control Dynam.*, vol. 39, no. 12, pp. 2776-2785, Dec. 2016, doi: 10.2514/1.G001795.

[15] K. Zeng, Y. Geng, and B. Wu, "Shape-based analytic safe trajectory design for spacecraft equipped with low-thrust engines," *Aerosp. Sci. Technol.*, vol. 62, pp. 87-97, Mar. 2017, doi:10.1016/j.ast.2016.12.006.

[16] A. Peloni, B. Dachwald, and M. Ceriotti, "Multiple near-Earth asteroid rendezvous mission: Solar-sailing options," *Adv. Space Res.*, vol. 62, no. 8, pp. 2084-2098, Oct. 2018, doi:10.1016/j.asr.2017.10.017.

[17] E. Vellutini, and G. Avanzini, "Shape-based design of low-thrust trajectories to cislunar Lagrangian point," *J. Guid. Control Dynam.*, vol. 37, no. 4, pp. 1329-1335, Jul. 2014, doi:10.2514/1.G000165.

[18] F. Jiang, G. Tang, and J. Li, "Improving low-thrust trajectory optimization by adjoint estimation with shape-based path," *J. Guid. Control Dynam.*, vol. 40, no. 12, pp. 3280-3287, Dec. 2017, doi: 10.2514/1.G002803.

[19] M. Bassetto, L. Niccolai, A. A. Quarta, and G. Mengali, "Logarithmic spiral trajectories generated by Solar sails," *Celest. Mech. Dyn. Astr.* vol. 130, no. 18, pp. 1-24, Feb. 2018, doi:10.1007/s10569-017-9812-6.

[20] O. Abdelkhalik, and E. Taheri, "Approximate on-off low-thrust space trajectories using Fourier series," *J. Spacecraft Rockets*, vol. 49, no. 5, pp. 962-965, Sep. 2012, doi: 10.2514/1.60045.

[21] E. Taheri, and O. Abdelkhalik, "Fast initial trajectory design for low thrust restricted-three-body problems," *J. Guid. Control Dynam.*, vol. 38, no. 11, pp. 2146-2160, Nov. 2015, doi: 10.2514/1.G000878.

[22] E. Taheri and O. Abdelkhalik, "Initial three-dimensional low-thrust trajectory design," *Adv. Space Res.*, vol. 57, no. 3, pp. 889-903, Feb. 2016, doi: 10.1016/j.asr.2015.11.034.

[23] E. Taheri, I. Kolmanovsky, and E. Atkins, "Shaping low-thrust trajectories with thrust-handling feature," *Adv. Space Res.*, vol. 61, no. 3, pp. 879-890, Feb. 2016, doi:10.1016/j.asr.2017.11.006.

[24] M. Huo, G. Zhang, N. Qi, Y. Liu and X. Shi, "Initial trajectory design of electric solar wind sail based on finite Fourier series shape-based method," *IEEE T. Aero. Elec. Sys*. 2019, doi: 10.1109/TAES.2019.2906050.

[25] M. Huo, G. Mengali, and A. A. Quarta, "Electric sail trajectory design with Bezier curve-based shaping approach," *Aerosp. Sci. Technol.*, vol. 88, pp. 126-135, Mar. 2019, doi: 10.1016/j.ast.2019.03.023.

[26] G. Farin, "Curves and Surfaces for Computer-Aided Geometric Design," *Practical Guide*, Ch. 4, pp. 44-46, 1997, doi: 10.2307/2008458.

[27] J. Kawaguchi, Y. Mimasu, O. Mori, R. Funase, T. Yamamoto, and Y. Tsuda, "IKAROS—Ready for Lift-Off as the World's First Solar Sail Demonstration in Interplanetary Space," *Proceedings of the 60th International Astronautical Congress*, Daejeon, Korea, 2009.

[28] M. Macdonald, G.W. Hughes, C.R. McInnes, A. Lyngvi, P. Falkner, and A. Atzei, "Solar polar orbiter: a solar sail technology reference study," *J. Spacecraft Rockets*, vol. 43, no. 5, pp. 960-972, Sep. 2006, doi: 10.2514/1.16408.

[29] H. Baoyin, and C. R. McInnes, "Solar sail equilibria in the elliptical restricted three-body problem," *J. Guid. Control Dynam.*, vol. 29 no. 3, pp. 538-543, May. 2006, doi: 10.2514/1.15596.

[30] S. Firuzi, and S. P. Gong, "Attitude control of a flexible solar sail in low Earth orbit," *J. Guid. Control Dynam.*, vol. 41, no. 8, pp. 1715-1730, Aug. 2018, doi: 10.2514/1.G003178.

[31] L. Niccolai, A. A. Quarta, and G. Mengali, "Solar sail trajectory analysis with asymptotic expansion method," Aerosp. Sci. Technol., Vol. 68, pp. 431-440, Sep. 2017, doi: 10.1016/j.ast.2017.05.038.

[32] P. Janhunen, "Electric sail for spacecraft propulsion," *J. Propul. Power*, vol. 20, no. 4, pp. 763-764, Jul.1998, doi:10.2514/1.8580

[33] G. Mengali, A. A. Quarta, and P. Janhunen, "Electric sail performance analysis," *J. Spacecraft Rockets*, vol. 45, no. 1, pp. 122-129, Jan. 2008, doi: 10.2514/1.31769.

[34] F. Liu, Q. Hu, and Y. Liu, "Attitude dynamics of electric sail from multibody perspective," *J. Guid. Control Dynam.*, vol. 41, no. 12, pp. 2633-2646, Dec. 2018, doi: 10.2514/1.G003625

[35] M. Huo, G. Mengali, and A. A. Quarta, "Electric sail thrust model from a geometrical perspective," *J. Guid. Control Dynam.*, vol. 41, no. 3, pp. 734-740, Mar. 2018, doi: 10.2514/1.G003169.

[36] L. Niccolai, A. A. Quarta, and G. Mengali, "Two-dimensional heliocentric dynamics approximation of an electric sail with fixed attitude," Aerosp. Sci. Technol., Vol. 71, pp. 441-446, Dec. 2017, doi: 10.1016/j.ast.2017.09.045.

[37] M. Bassetto, G. Mengali, and A. A. Quarta, "Thrust and torque vector characteristics of axially- symmetric E-sail", Acta Astronaut., Vol. 146, pp. 134-143, May 2018, doi:10.1016/j.actaastro.2018.02.035.

[38] M. Zubrin, and G. Andrews, "Magnetic sails and interplanetary travel," *J. Spacecraft Rockets*, vol. 28, no. 2, pp. 197-203, Mar. 1991, doi: 10.2514/3.26230.

[39] M. Bassetto, A. A. Quarta, and G. Mengali, "Magnetic sail-based displaced non-Keplerian orbits", Aerosp. Sci. Technol., Vol. 92, pp. 363–372, Sep. 2019, doi:10.1016/j.ast.2019.06.018.

[40] Y. Tsuda, O. Mori, R. Funase, H. Sawada, T. Yamamoto, T. Saiki, T. Endo, and J. Kawaguchi, "Flight status of IKAROS deep space solar sail demonstrator," *Acta Astronaut*., vol. 69, no. 9_10, pp. 833-840, Nov. 2011, doi: 10.1016/j.actaastro.2011.06.005.

[41] Y. Mimasu, T. Yamaguchi, M. Matsumoto, M. Nakamiya, R. Funase, and J. Kawaguchi, "Spinning solar sail orbit steering via spin rate control," *Adv. Space Res.*, vol. 48, no. 11, pp. 1810-1821, Dec. 2011, doi: 10.1016/j.asr.2011.08.030.

[42] G. Aliasi, G. Mengali, and A. A Quarta, "Artificial Lagrange points for solar sail with electrochromic material panels," *J. Guid. Control Dynam.*, vol. 36, no. 5, pp. 1544-1550, Sep. 2013, doi: 10.2514/1.58167.

[43] J. Mu, S. Gong, and J. Li, "Reflectivity-controlled solar sail formation flying for magnetosphere mission," *Aerosp. Sci. Technol.*, vol. 30, no. 1, pp. 339-348, Oct. 2013, doi: 10.1016/j.ast.2013.09.002.

[44] J. Mu, S. Gong, and J. Li, "Coupled control of reflectivity modulated solar sail for GeoSail formation flying," *J. Guid. Control Dynam.*, vol. 38, no. 4, pp. 740-751, Apr. 2015, doi: 10.2514/1.G000117.

[45] S. Gong, and J. Li, "Orbital motions of a solar sail around the L2 Earth-Moon libration point," *J. Guid. Control Dynam*., vol. 37, no. 4, pp. 1349-1356, Jul. 2014, doi: 10.2514/1.G000063.

[46] S. Gong, and J. Li, "Solar sail halo orbit control using reflectivity control devices," *T. Jpn. Soc. Aeronaut. S.* vol. 57, no. 5, pp. 279-288, Sep. 2014, doi: 10.2322/tjsass.57.279.

[47] S. Gong, and J. Li, "Equilibria near asteroids for solar sails with reflection control devices," *Astrophys Space Sci*., vol. 355, pp. 213-223, Dec. 2015, doi: 10.1007/s10509-014-2165-7.

[48] D. Benson, "A gauss pseudospectral transcription for optimal control," PhD thesis, MA Institute of Technology, 2005.